Constraints on the Skyrme Equations of State from Properties of Doubly Magic Nuclei

B. Alex Brown

Department of Physics and Astronomy and National Superconducting Cyclotron Laboratory, Michigan State University, East Lansing, Michigan 48824-1321, USA

(Received 14 August 2013; published 3 December 2013)

I use properties of doubly magic nuclei to constrain symmetric nuclear matter and neutron matter equations of state. I conclude that these data determine the value of the neutron equation of state at a density of $\rho_{on} = 0.10$ nucleons/fm^3 to be 11.4(10) MeV. The slope at that point is constrained by the value of the neutron skin. Analytical equations are given that show the dependence of the Skyrme equations of state on the neutron skin.

DOI: 10.1103/PhysRevLett.111.232502 PACS numbers: 21.10.Dr, 21.10.Pc, 21.30.Fe, 21.60.Cs

The neutron equation of state (EOS) is important for understanding properties of neutron stars [1,2]. Recently an extensive study was made of the constraints on the Skyrme energy-density functionals (EDFs) provided by the properties of nuclear matter [3]. Out of several hundred Skyrme EDFs, the 16 given in Table VI of [3], called the CSkP set, best reproduced a selected set of experimental nuclear matter properties. Five of these were eliminated [3] since they gave transitions to spin-ordered matter around $\rho = 0.25$ fm^{-3}. The remaining 11 are those given in Table I and labeled with their name and order in Table VI of [3]. I start with these 11 interactions and use properties of doubly magic nuclei to provide further constraints on the deduced EOS. I also consider the SLy4 [4] and SkM* [5] EDFs since they are widely used in the literature.

The EOS for symmetric nuclear matter (SNM), neutron matter, and the symmetry energy S obtained with the CSkP, SLy4, and SkM* parameters given in Table VI of [3] are shown in Fig. 1(a). The symmetry energy EOS is the difference between the neutron EOS and matter EOS. The spread is relatively small, but I will demonstrate that the spread can be reduced if the Skyrme parameters are constrained by the same set of nuclear data. I will also show that there is a crossing point in the neutron EOS that has a value that is independent of a reasonable uncertainty in the neutron rms radius of ^{208}Pb. Finally, I give analytic formulas that show how the Skyrme EOS depends upon the neutron rms of ^{208}Pb.

The data set consists of the following ground-state properties of the doubly magic nuclei used for the Skx family of Skyrme interactions [6–10]: ^{16}O, ^{24}O, ^{34}Si ^{40}Ca, ^{48}Ca, ^{48}Ni, ^{68}Ni, ^{88}Sr, ^{100}Sn, ^{132}Sn, and ^{208}Pb. The properties are binding energies, rms charge radii, and single-particle energies. These data are given in [6]. All of the CSkP functionals were constrained to have a range of L values (defined below) that correspond to a neutron skin thickness (the differences between the neutron and proton rms radii) for ^{208}Pb to be near $R_{np} = 0.20$ fm. The Ska25s20 and Ska35s20 are unpublished functionals in the Skx family that were constrained to have $R_{np} = 0.20$ fm. I start by constraining the skin thickness to be exactly $R_{np} = 0.20$ fm. This constraint will later be relaxed. The Skx family drops the Coulomb exchange term in order to reproduce the binding energy differences between ^{48}Ni and ^{48}Ca [7].

Starting with the parameters given in Table VI of [3], I refit t_0, t_1, t_2, t_3, x_0 and x_3 to the doubly magic data for each case (the spin orbit strength W is also fit). The functional forms for the Skyrme EDF and its nuclear matter properties are given in [3]. These parameters are all well determined by the data set. The values for σ, x_1, and x_2 were fixed at their original values. A reasonable range of σ gives relatively good fits to the data. The x_1 and x_2 are not determined from the data. The parameters that are fixed are given in Table I together with the value of the χ^2 of the fit. The fourth one in Table VI of [3] (LNS) was not used since it did not give converged results for nuclei. The new results for the EOS are shown in Fig. 1(b). The EOS are now more tightly constrained. The single-particle energies included in the fit are best reproduced with a nuclear-matter effective mass of near unity. The fit quickly converges for the values of the binding energies and radii. The convergence for single-particle energies is an order of magnitude slower. If all of the fits were fully converged, they would end up with a lower χ^2 value and with SNM effective masses near unity. I stop with the quick convergence part that leaves some range of values for the SNM effective mass.

Some of the CSkP set were eliminated in [3] because the neutron matter effective mass was not less than unity. However, I find that by repeating the fit and allowing the x_1 parameter to vary and keeping x_2 fixed, the neutron effective mass at $\rho_{on} = 0.10$ fm^{-3} can be fixed at a value of 0.90 without any significant change to the χ^2 for the fit to nuclear ground-state data. (The neutron effective mass depends upon both x_1 and x_2. In some cases x_2 can be varied and x_1 can be fixed. In the case of Sly4 it was only possible to do the latter.) The EOS are shown in Fig. 2(a). They are similar to those in Fig. 1(b), but are closer

TABLE I. Properties of the fitted Skyrme interactions with $R_{np} = 0.20$ fm. The results for x_1 in the last column were obtained with the additional constraint that $m_n^*(\rho_{on})/m \approx 0.90$. (b) are the six best-fit results shown by the black lines in the figures.

Name		σ	x_1	x_2	χ^2	K_m (MeV)	m_n^*/m at $\rho_{on} = 0.10$ fm^{-3}	m^*/m at $\rho_{om} = 0.16$ fm^{-3}	x_1
KDE0v1	s3	1/6	−0.35	−0.93	1.88	219	0.79	0.79	0.18
LNS	s4	1/6	0.06	0.66					
NRAPR	s6	0.14	−0.05	0.03	2.77	227	1.00	0.85	−0.07
Ska25s20	s7	0.25	−0.80	0.00	0.88 (b)	219	0.99	0.99	−1.35
Ska35s20	s8	0.35	−0.80	0.00	0.74 (b)	240	1.00	1.00	−1.46
SKRA	s9	0.14	0.00	0.20	1.70	215	0.99	0.79	−0.45
SkT1	s10	1/3	−0.50	−0.50	0.79 (b)	236	0.98	0.97	−1.02
SkT2	s11	1/3	−0.50	−0.50	0.82 (b)	237	0.95	0.97	−0.99
SkT3	s12	1/3	−1.00	1.00	0.76 (b)	236	0.98	0.98	−1.52
SQMC700	s15	1/6	0.00	0.00	2.50	227	0.92	0.71	−0.08
SV-sym32	s16	0.30	−0.59	−2.17	0.83 (b)	233	1.12	0.91	−1.77
SLy4	s17	1/6	−0.34	−1.00	3.42	230	0.73	0.70	
SkM*	s18	1/6	0.00	0.00	1.71	221	0.98	0.78	−0.36

together at large density. The resulting x_1 values are given on the right-hand side of Table I. A good fit would be obtained for a reasonably wide range of values for the neutron effective mass at $\rho_{on} = 0.10$ fm^{-3} (0.8 to 1.0). The average deviation for the binding energies was always less than one MeV. The average deviation for the best fit was about 0.5 MeV. The largest deviation was always that for ^{24}O which was up to three MeV (1.8% in the binding energy).

The CSkP sets provide a reasonable range of values for SNM incompressibility K_m from 219 to 240 MeV as given in Table I. The fit to nuclear ground-state data is good for all of this range. The range of values obtained from a quasi-particle random-phase approximation analysis of the giant monopole resonance is 217–230 MeV [11].

The fits are then performed with constraints of $R_{np} = 0.16$ and $R_{np} = 0.24$ fm. The results are shown in Fig. 2(b). The χ^2 values are similar for this range of R_{np}. The average deviation for the binding energies was similar for $R_{np} = 0.16$ and $R_{np} = 0.20$ fm, but increased by 0.1–0.3 MeV for $R_{np} = 0.24$ fm.

The neutron EOS for these two fits cross at values from $\rho = 0.096$ to $\rho = 0.104$ fm^{-3}, indicating that the value of the neutron EOS is most well determined in this range. I take the average value of $\rho_{on} = 0.10$ fm^{-3} to define the point at which the value of the neutron EOS is most well determined. This crossing point is more precise than that found in [12] because none of the Skyrme functionals considered there, except for Skx, were fit to a consistent set of ground state data for doubly magic nuclei. The average neutron density for the interior of ^{208}Pb is about $\rho_n = (126/208)(\rho_{om}) = 0.097$ with $\rho_{om} = 0.16$ fm^{-3}.

The values of the neutron EOS at $\rho_{on} = 0.10$ fm^{-3} range from 10.5 to 12.2 MeV. When the fits were repeated with the constraint that $m_n^*/m = 1.0$, the results for E/N at $\rho_n = 0.10$ fm^{-3} increased by an average of 0.2 MeV. Taking all of this into account, we have a mean value of E/N $(\rho_n = 0.10$ fm$^{-3}) = 11.4(10)$ MeV for the entire CSkP set, and 10.9(5) MeV for the six best-fit results (the black lines in the figures).

The low-density results for the neutron EOS are shown in Fig. 3 for the three values of R_{np}. They are compared with the upper and lower values from the blue error band shown in Fig. 8 of [14] for calculations based on the Entem and Machleidt N^{3}LO potential with a cutoff at 500 MeV that include N^{2}LO NNN forces from [13] (the dashed lines in Fig. 3). Other predictions are shown in Fig. 7 of [14]. The present results for $R_{np} = 0.20$ fm are most consistent with the theoretical error band. The present results will be important for comparing to future calculations with smaller error bands.

All of the curves obtained by Skyrme EDF in these figures are given by the analytical expression

$$F(\rho) = a\rho + b\rho^{\gamma} + c\rho^{2/3} + d\rho^{5/3}, \tag{1}$$

where $\gamma = 1 + \sigma$, and a, b, c, and d are constants that depend on the Skyrme parameters. The first term is from the delta-function part that depends on t_0 and x_0, the second term is from the density-dependent part that depends on t_3 and x_3, the third term is the Fermi-gas kinetic energy, and the fourth term depends on t_1, t_2, x_1, and x_2. The effective mass is given by

$$\frac{m^*(\rho)}{m} = \frac{c}{c + d\rho}. \tag{2}$$

The first and second derivatives are given by

$$F'(\rho) = a + b\gamma\rho^{\gamma-1} + (2/3)c\rho^{-1/3} + (5/3)d\rho^{2/3} \tag{3}$$

and

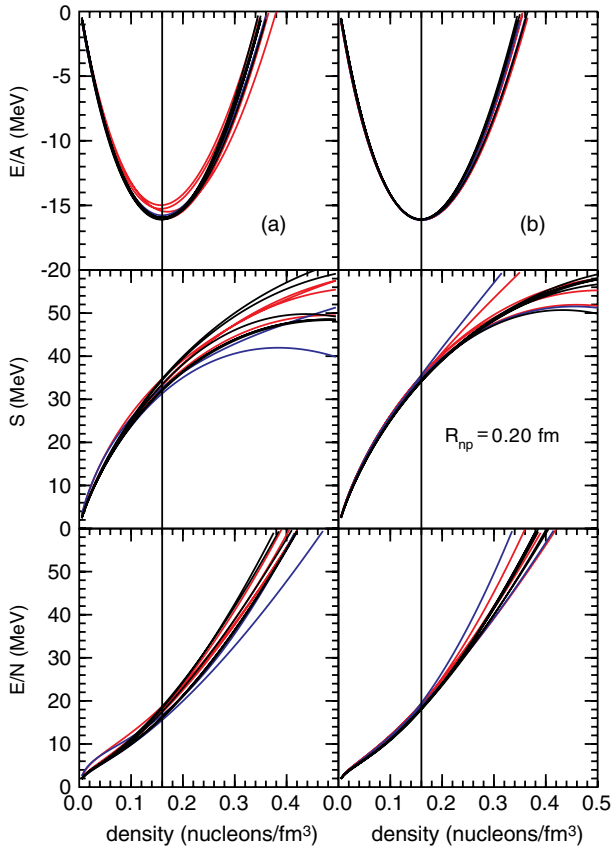

FIG. 1 (color online). (a) EOS obtained from the Skyrme interactions. (b) EOS obtained from the Skyrme interactions fitted to properties of doubly magic nuclei and with a constraint of $R_{np} = 0.20$ fm for the neutron skin of ^{208}Pb. The black lines are those from the CSkP set with $m^*/m \approx 1.0$, the red lines are those from the CSkP set with $m^*/m = 0.70$–0.85. The blue lines are those for SLy4 and SkM*. The vertical line is placed at $\rho = 0.16$ fm^{-3}.

$$F''(\rho) = \gamma(\gamma-1)b\rho^{\gamma-2} - (2/9)c\rho^{-4/3} + (10/9)d\rho^{-1/3}. \quad (4)$$

Given a fixed c and d one can write

$$[F(\rho)/\rho] = a + b\rho^{\gamma-1} + A(\rho) \quad (5)$$

and

$$F'(\rho) = a + b\gamma\rho^{\gamma-1} + B(\rho), \quad (6)$$

where

$$A(\rho) = c\rho^{-1/3} + d\rho^{2/3} \quad (7)$$

and

$$B(\rho) = (2/3)c\rho^{-1/3} + (5/3)d\rho^{2/3}. \quad (8)$$

These equations provide the results needed to obtain a and b in terms of $F(\rho_o)$ and $F'(\rho_o)$ at a fixed point $\rho = \rho_o$,

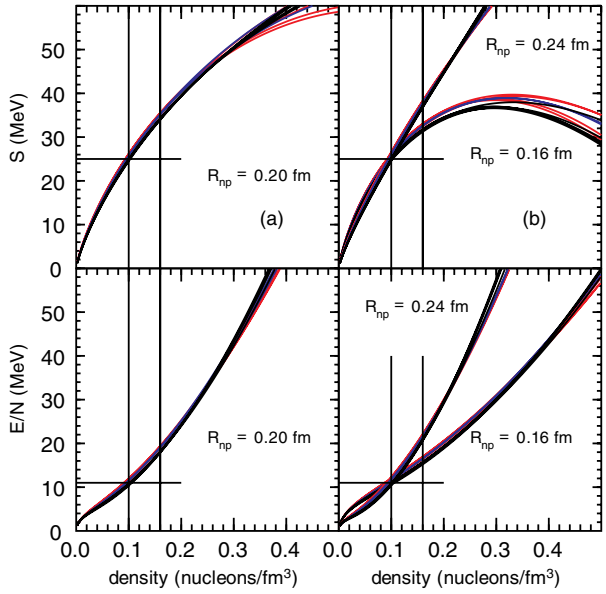

FIG. 2 (color online). (a) EOS obtained from the Skyrme interactions fitted to properties of doubly magic nuclei with 0.20 fm for the neutron skin of ^{208}Pb and $m_n^*/m = 0.90$ at $\rho_{on} = 0.10$ fm^{-3}. (b) EOS obtained from the Skyrme interactions fitted to properties of doubly magic nuclei with values of 0.16 and 0.24 fm for the neutron skin of ^{208}Pb together with $m_n^*/m = 0.90$. See caption to Fig. 1. The vertical lines are placed at $\rho = 0.10$ and 0.16 fm^{-3}. The horizontal lines are placed at 25 MeV for S and 11 MeV for E/N.

$$b = \frac{F'(\rho_o) - [F(\rho_o)/\rho_o] + A(\rho_o) - B(\rho_o)}{(\gamma-1)\rho_o^{\gamma-1}}, \quad (9)$$

and

$$a = [F(\rho_o)/\rho_o] - b\rho_o^{\gamma-1} - A(\rho_o). \quad (10)$$

It is conventional to define the value and derivatives at $\rho_{om} = 0.16$ fm^{-3} with $J = F(\rho_{om})$, $L = 3\rho_{om}F'(\rho_{om})$ and $K = 9\rho_{om}^2F''(\rho_{om})$.

There are two independent EOS, one for the SNM EOS, $F_m = (E/A)$ with $c_m = 75$ MeV fm^2, and another for the neutron EOS, $F_n = (E/N)$ with $c_n = 119$ MeV fm^2 (the values for c are from the Fermi-gas model). From these two functions one obtains the symmetry energy, $S = F_{\rm sym} = F_n - F_m$, with $a_{\rm sym} = a_n - a_m$, etc. J and L are usually associated with $F_{\rm sym,}$ although they can be also be applied to F_m and F_n (e.g., $J_{\rm sym} = J_n - J_m$). The equations above provide analytical forms for the correlations between a, b, d, γ, J, L, K, $F(\rho_o)$ and $F'(\rho_o)$.

For a given γ and effective mass (d), the values of $F(\rho_o)$ and $F'(\rho_o)$ determine the entire EOS. For example, with $\gamma = 1.25$ and an effective mass of unity for the SNM EOS ($d_m = 0$ MeV fm^5), the well-established values $F_m(\rho_{om}) = -16.0$ MeV, $F'_m(\rho_{om}) = 0.0$ MeV fm^3 lead to $b_m = -924$ MeV fm$^{3\gamma}$ [Eq. (9)], $a_m = 822$ MeV fm^3 [Eq. (10)], and $K_m = 219$ MeV [Eq. (4)]. With Eq. (1), this

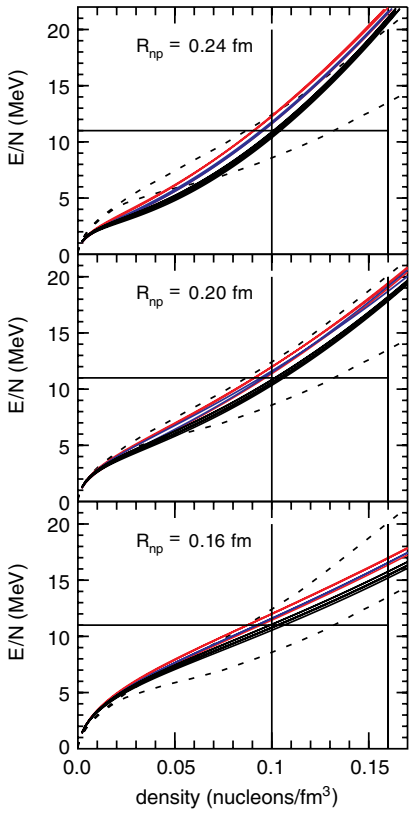

FIG. 3 (color online). The neutron EOS at low density for $R_{np} = 0.16$, 0.20, and 0.24 fm. They are compared to the theoretical results from [14] (dashed lines). See caption to Fig. 1. The vertical lines are placed at $\rho = 0.10$ and 0.16 fm^{-3}. The horizontal line is placed at 11 MeV.

provides a SNM EOS that is within the error band of those shown in the top part of Fig. 1.

For neutron matter we have $F_n(\rho_{on}) = (E/N)(\rho_{on}) = 11.4(10)$ MeV at $\rho_{on} = 0.10$ fm^{-3}. The symmetry energy at this point is $S(\rho_{on}) = F_n(\rho_{on}) - F_m(\rho_{on}) = 11.4(10) + 14.1(1) = 25.5(10)$ MeV. The value $S(\rho_{on})$ derived from nuclear binding enegies is consistent with the value of $S(\rho_{on}) = 24.1(8)$ MeV found from an analysis of the energy of the giant dipole resonance in ^{208}Pb [15]. The derivative of the symmetry energy at $\rho_{on} = 0.10$ fm^{-3} is approximately linear with the value of R_{np} with

$$S'(\rho_{on}) = p_a R_{np}, \tag{11}$$

and

$$F_n'(\rho_{on}) = S'(\rho_{on}) + F_m'(\rho_{on}) = p_a R_{np} + p_b, \tag{12}$$

with $p_a = 882(32)$ MeV fm^2 and $p_b = -70(2)$ MeV fm^3 (p_a was obtained from the 36 curves shown in Fig. 2, where the lowest value was 850 MeV fm^2 and the highest value was 915 MeV fm^2. The value for p_b is obtained from the SNM EOS at $\rho_{on} = 0.10$ fm^{-3}.) Equation (12) is consistent with the theoretical data shown in Fig. 3 of [12] and Fig. 1 of [16]. In [17], F_n' is related to R_{np} with an expansion up to a quadratic around $\rho_{om} = 0.16$ fm^{-3}. The result of Eq. (12) is simpler because it is expanded around $\rho_{on} = 0.10$ fm^{-3}, the point at which the value of F_n is fixed.

For a given value of R_{np} we have F_n' from Eq. (12) that can be used to obtain a_n and b_n. For example, $R_{np} = 0.20$ fm gives $F_n'(\rho_{on}) = 106$ MeV fm^3. Then with $\gamma = 1.25$, an effective mass of $[m_n^*/m](\rho_{on}) = 0.90$ [$d_n = 124$ MeV fm^5 from Eq. (2)], and $F_n(\rho_{on}) = 11.4$ MeV, we obtain $b_n = 424$ MeV fm$^{3\gamma}$ [Eq. (9)] and $a_n = -408$ MeV fm^3 [Eq. (10)]. With Eq. (1), this provides a neutron matter EOS that is within the error band of those shown on the left-hand side of Fig. 2. Equations (1)–(4) with $a_{\rm sym} = a_n - a_m$, etc., given above can be used to obtain $J_{\rm sym} = 34.6$ MeV, $L_{\rm sym} = 64.7$ MeV, $K_{\rm sym} = -109$ MeV.

Although the $\gamma = 1 + \sigma$ value and the d term are not the same for all of the Skyrme EDFs considered, all of the lines in Figs. 2 and 3 are within a narrow band. An assumption for all of the Skyrme EDFs considered is that $\gamma = 1 + \sigma$ is the same for both the SNM and neutron EOS. The γ for SNM is constrained by the K_m value obtained from the energy of the giant monopole resonance. The value of γ may be different for neutron matter, and this would affect the $K_{\rm sym}$ value and extrapolation of the neutron EOS to higher density. The ^{208}Pb neutron skin thickness obtained from the PREX parity-violating electron scattering experiment is $R_{np} = 0.302 \pm (0.175)_{\rm exp} \pm (0.026)_{\rm model} \pm (0.005)_{\rm strange}$ fm [18,19]. A PREX-II experiment has been approved that is expected to reduce the error bar to about 0.06 fm. This will put an important constraint on the neutron EOS. Other data that will constrain the neutron EOS come from properties of the dipole resonance [20,21] and from nuclear reactions [22].

This work was inspired by presentations and conversations during the International Collaborations in Nuclear Theory (ICNT) Program on "Symmetry Energy in the Context of New Radioactive Beam Facilities and Astrophysics" held at the National Superconducting Cyclotron Laboratory, July 15–August 9, 2013. I was supported by NSF Grant No. PHY-1068217.

[1] A. W. Steiner, J. M. Lattimer, and E. F. Brown, Astrophys. J. **765**, L5 (2013).
[2] A. W. Steiner, M. Prakash, J. M. Lattimer, and P. J. Ellis, Phys. Rep. **411**, 325 (2005).
[3] M. Dutra, O. Lourenco, J. S. Sa Martins, A. Delfino, J. R. Stone, and P. D. Stevenson, Phys. Rev. C **85**, 035201 (2012).
[4] E. Chabanat, P. Bonche, P. Haensel, J. Meyer, and R. Schaeffer, Nucl. Phys. **A635**, 231 (1998).
[5] J. Bartel, P. Quentin, M. Brack, C. Guet, and H. B. Hakansson, Nucl. Phys. **A386**, 79 (1982).
[6] B. A. Brown, Phys. Rev. C **58**, 220 (1998).

[7] B. A. Brown, W. A. Richter, and R. Lindsay, Phys. Lett. B **483**, 49 (2000).
[8] B. A. Brown, T. Duguet, T. Otsuka, D. Abe, and T. Suzuki, Phys. Rev. C **74**, 061303(R) (2006).
[9] B. A. Brown, G. Shen, G. C. Hillhouse, J. Meng, and A. Trzcinska, Phys. Rev. C **76**, 034305 (2007).
[10] B. A. Brown, A. Derevianko, and V. V. Flambaum, Phys. Rev. C **79**, 035501 (2009).
[11] L. G. Cao, H. Sagawa, and G. Colo, Phys. Rev. C **86**, 054313 (2012).
[12] B. A. Brown, Phys. Rev. Lett. **85**, 5296 (2000)
[13] K. Hebeler and A. Schwenk, Phys. Rev. C **82**, 014314 (2010).
[14] T. Kruger, I. Tews, K. Hebeler, and A. Schwenk, Phys. Rev. C **88**, 025802 (2013).
[15] L. Trippa, G. Colo, and E. Vigezzi, Phys. Rev. C **77**, 061304(R) (2008).
[16] S. Typel and B. A. Brown, Phys. Rev. C **64**, 027302 (2001).
[17] S. Yoshida and H. Sagawa, Phys. Rev. C **73**, 044320 (2006).
[18] S. Abrahamyan, Z. Ahmed, H. Albataineh, K. Aniol, D. S. Armstrong, W. Armstrong, T. Averett, B. Babineau, A. Barbieri, V. Bellini *et al.*, Phys. Rev. Lett. **108**, 112502 (2012).
[19] C. J. Horowitz, Z. Ahmed, C.-M. Jen, A. Rakhman, P. A. Souder, M. M. Dalton, N. Liyanage, K. D. Paschke, K. Saenboonruang, R. Silwal *et al.*, Phys. Rev. C **85**, 032501 (2012).
[20] P. G. Reinhard and W. Nazarewicz, Phys. Rev. C **81**, 051303 (2010).
[21] X. Roca-Maza, M. Brenna, G. Colo, M. Centelles, X. Vinas, B. K. Agrawal, N. Paar, D. Vretenar, and J. Piekarewicz, Phys. Rev. C **88**, 024316 (2013).
[22] M. B. Tsang, Y. Zhang, P. Danielewicz, M. Famiano, Z. Li, W. G. Lynch, and A. W. Steiner, Phys. Rev. Lett. **102**, 122701 (2009).